Solution of the point kinetics equations in the presence of Newtonian temperature feedback by Padé approximations via the analytical inversion method

A E Aboanber and A A Nahla

Department of Mathematics, Faculty of Science, Tanta University, Tanta, 31527, Egypt

E-mail: aboanber@dec1.tanta.edu.eg

Abstract
A method based on the Padé approximations is applied to the solution of the point kinetics equations with a time varying reactivity. The technique consists of treating explicitly the roots of the inhour formula. A significant improvement has been observed by treating explicitly the most dominant roots of the inhour equation, which usually would make the Padé approximation inaccurate. Also the analytical inversion method which permits a fast inversion of polynomials of the point kinetics matrix is applied to the Padé approximations. Results are presented for several cases of Padé approximations using various options of the method with different types of reactivity. The formalism is applicable equally well to non-linear problems, where the reactivity depends on the neutron density through temperature feedback. It was evident that the presented method is particularly good for cases in which the reactivity can be represented by a series of steps and performed quite well for more general cases.

PACS numbers: 02.30.Mv, 28.20.−v

1. Introduction

In a previous work [1] the analytical inversion method that permits a fast inversion of polynomials of the point kinetics matrix was introduced. The method was applied to different cases of Padé approximations as a solution of reactor dynamics with a step input of reactivity.

In the form considered here, the point reactor kinetics equations are a system of coupled non-linear ordinary differential equations. Included in the system are equations which describe the neutron level, time-dependent reactivity, an arbitrary number of delayed neutron groups and any thermodynamics variables that enter into the reactivity equation. These equations are used to describe the power as neutronic properties of the internal elements of a nuclear reactor that change with time. This would include the motion of control rods, the motion of

fuel material in an accident scenario, the loss of coolant as the reactor undergoes a blow-down accident and additional material motion. The equations are formulated as a set (usually of seven) of ordinary differential equations that can exhibit a rather stiff solution (widely spaced eigenvalues). Except for a few special cases, it is not possible to obtain closed solutions to these equations in terms of elementary functions because of a time-dependent reactivity and the stiffness. The time dependence makes it difficult to obtain an analytical solution, and thus a numerical integration is usually employed [2, 3]. The stiffness of the kinetics equations, however, restricts the time step to a small increment, making the numerical solution very inefficient [2–5]. Several methods have been proposed to overcome this difficulty [2, 4, 5], but they do not seem fully satisfactory because of their lack of accuracy, generality and/or simplicity. In the previous work the analytical approach based on the analytical inversion method, which has a direct applicability on the Padé approximation, has been introduced [1]. This method provides a fast and an accurate computational technique for the point kinetics equations with step reactivity and a large time increment (time step) compared to the other conventional methods.

The aim of this work is to apply the analytical inversion method to the solution of the point reactor kinetics equations using different types of Padé approximations and time-dependent reactivity with temperature feedback. The presence of temperature feedback is useful in providing an estimate of the transient behaviour of a reactor power and of other system variables in a reactor core, which are fairly tightly coupled.

Many authors have treated the problem of reactivity feedback for the point kinetics equations. Frohlich and Johnson [6] obtained a solution using a constant heat removal model for a ramp input of reactivity. Russel and Duncan [7] have recently used a similar model for investigating non-adiabatic excursions for a large step input of reactivity. Recently, the asymptotically stable solution for the neutron density in the point-reactor kinetics equations was obtained by Gupta [8] for a step input of reactivity in the presence of m groups of delayed neutrons. March-Leuba *et al* [9] have shown that a phenomenological model that retains the essential physical processes dominating the dynamics behaviour of a BWR can be described by a one-point representation of the reactor kinetics, a one-point representation of the heat transfer process in the fuel and two-node representations of the channel thermal hydraulics to account for the void reactivity feedback.

In section 2 a review of the basic procedure for the solution for the point kinetics equations with time varying reactivity is presented. Section 3 includes applications of different types of Padé approximations to this solution. Numerical results are discussed in section 4 and the conclusion comes finally in section 5.

2. General solution of the reactor kinetics equations

In the space-average approximation, the differential equations of the point-reactor kinetics equations with G groups of delayed neutrons in terms of the generation time may be written as

$$\frac{dN(t)}{dt} = \frac{\rho(t) - \beta}{\Lambda} N(t) + \sum_{i=1}^{G} \lambda_i C_i(t) + S(t) \tag{1}$$

$$\frac{dC_i(t)}{dt} = \frac{\beta_i}{\Lambda} N(t) - \lambda_i C_i(t) \qquad i = 1, 2, \ldots, G \tag{2}$$

and the Newtonian feedback from the fuel temperature can be written as

$$\left.\begin{aligned}\frac{\mathrm{d}T(t)}{\mathrm{d}t} &= KN(t) - \gamma(T - T_c)\\ \rho(t) &= I(t) + b[T(t) - T_0]\end{aligned}\right\} \tag{3}$$

where

$N(t)$ and $C_i(t) \equiv$ weighted integrals of the neutron density and ith precursor concentrations $(i = 1, 2, \ldots, G)$
$S(t) \equiv$ source term
$\rho(t) \equiv$ net reactivity
$\beta, \beta_i, \lambda_i \equiv$ delayed neutron constants $(i = 1, 2, \ldots, G)$, where G is the total number of delayed neutron groups
$T(t)$, T_0 and $T_c \equiv$ the temperature of the reactor at time t, zero and effective coolant temperature, respectively
$K \equiv$ the reciprocal of the reactor heat capacity and $(1/\gamma)$ is interpreted as the mean time for heat transfer to the coolant
$\Lambda \equiv$ neutron generation time
$b \equiv$ the temperature coefficient of reactivity
$I(t) \equiv$ the impressed reactivity

Anticipating a very short time scale for the excursion, we ignore heat loss when the time constant for heat transfer $(1/\gamma)$ is very large compared to the time scale of the excursion and use the adiabatic model as

$$\left.\begin{aligned}\frac{\mathrm{d}T(t)}{\mathrm{d}t} &= KN(t)\\ \rho(t) &= I(t) + b[T(t) - T_0]\end{aligned}\right\}. \tag{3a}$$

The reactivity $\rho(t)$ is represented in generalized notation

$$\rho(t) = I(t) + F(t) \tag{4}$$

where $F(t)$ is a function representing the reactivity feedback. For example, $I(t)$ may have the form $\sin(\omega t)$, $\exp(\omega t)$, or a polynomial in t, while $F(t)$ may be a function of temperature, power level, density or other variables. Assume a shutdown effect proportional to integrated neutron density (which in turn is proportional to fission energy release for a given Λ). Since all calculations started from initial equilibrium with $N(0) = 1$ neutron/cm^3 the compensated reactivity $\rho(t)$ is represented, equation $(3a)$, as

$$\rho(t) = I(t) + P(t) \int_0^t N(t') \, \mathrm{d}t' \tag{5}$$

where $P(t)$ is the shutdown coefficient of the reactor system ranging from $\sim 10^{-13}$ cm^3 s^{-1} for slow systems to $\sim 10^{-7}$ cm^3 s^{-1} for fast metal systems. However, it will not be necessary to specify the explicit form of $\rho(t)$ until a specific problem is considered.

Equations (1) and (2) can be rewritten in matrix form as

$$\frac{\mathrm{d}\Psi(t)}{\mathrm{d}t} = A(t)\Psi(t) + S(t) \tag{6}$$

where

$$\begin{aligned}\Psi(t) &= \mathrm{col}[N(t) \quad C_1(t) \quad \cdots \quad C_G(t)]\\ &= \mathrm{col}[\Psi_1(t) \quad \Psi_2(t) \quad \cdots \quad \Psi_{G+1}(t)]\\ \mathbf{S}(t) &= \mathrm{col}[S(t) \quad 0 \quad \cdots \quad 0]\end{aligned}$$

and

$$\mathbf{A}(t) = \begin{bmatrix} \dfrac{\rho(t) - \beta}{\Lambda} & \lambda_1 & \lambda_2 & \cdots & \lambda_G \\[1.2em] \dfrac{\beta_1}{\Lambda} & -\lambda_1 & 0 & \cdots & 0 \\[1.2em] \dfrac{\beta_2}{\Lambda} & 0 & -\lambda_2 & \cdots & 0 \\[1.2em] \vdots & \vdots & \vdots & \ddots & \vdots \\[1.2em] \dfrac{\beta_G}{\Lambda} & 0 & 0 & \cdots & -\lambda_G \end{bmatrix} = [\mathbf{a}_{ij}]$$

denotes a $G + 1 \times G + 1$ matrix. In most cases the extraneous source contributions are negligible, so that $\mathbf{S}(t) = 0$ [10][1].

   If the reactivity ρ is constant, it is easy to verify that the exact solution of equation (6) is

$$\Psi(t) = \exp[\mathbf{A}\,t]\Psi(0).$$

In particular, if Ψ_n and Ψ_{n+1} denote the solution at times t_n and $t_{n+1} = t_n + \Delta t$, respectively, then

$$\Psi_{n+1} = \exp[\mathbf{A}\,\Delta t]\Psi_n. \tag{7}$$

   If the reactivity ρ (and thus the matrix $\mathbf{A}$) is a function of time, then equation (7) will no longer give the solution for equation (6). However, equation (7) suggests a form that should be quite suitable for generating an approximate solution of the more general problem (time-dependent problem). The variation in reactivity over the interval $[t_{n+1}, t_n]$ is accounted for by replacing the exponential argument in equation (7) by the average of $\mathbf{A}(t)$ at t_n and t_{n+1}. That is, equation (7) is generalized to read

$$\Psi_{n+1}^* = \exp\left[\frac{(\mathbf{A}_n + \mathbf{A}_{n+1})}{2}\Delta t\right]\Psi_n^* \tag{8}$$

where Ψ_n^* is now an approximation to the exact solution Ψ_n. Note that equation (8) would be reduced to equation (7) if $\mathbf{A}$ is a constant matrix. The local discretization error of the method has been estimated [1] and was found to be in the order of $O(\Delta t)^3$.

   To enhance the method of calculations we have developed a purification method [1] based on an approximate expression for $\exp(\mathbf{A}\,\Delta t)$ with the explicit treatment of the real roots of the inhour equation. This method was found to be very fast and accurate and has the ability to reproduce all the feature of transients, including the prompt jump, and will be summarized here.

   The approximate expression of the exponential matrix $\mathbf{A}$ or generally $(\mathbf{A}\,\Delta t)$ is

$$\exp(\mathbf{A}\,\Delta t) = f(\mathbf{A}\,\Delta t) + \sum_{i=0}^{G} [\exp(\Delta t\omega_i) - f(\Delta t\omega_i)]\mathbf{U}_i\mathbf{V}_i^T \tag{9}$$

where $\mathbf{U}_i$ and $\mathbf{V}_i$ are the eigenvectors of the matrices $\mathbf{A}$ and $\mathbf{A}^T$, respectively, which form a biorthonormal set when properly normalized [11], so $V_i^T U_k = \delta_{ik}$. We should note that, if $f(\Delta t\,\omega_i)$ is a good approximation for $\exp(\Delta t\,\omega_i)$, we are justified in dropping the ith term from the summation. It will have a very small coefficient, namely,

$$[\exp(\Delta t\,\omega_i) - f(\Delta t\,\omega_i)] \prec\prec 1. \tag{10}$$

[1] At very low flux, as in reactor startup, the source perturbation on kinetic behaviour can be appreciable. However, many reactor control problems are concerned with power levels at which source perturbation is negligible.

Since $\exp(\Delta t\, \omega_i) \approx f(\Delta t\, \omega_i)$, thus, to a high degree of accuracy, we have

$$\exp(\Delta t\, \mathbf{A}) \cong g(\Delta t\, \mathbf{A}) = f(\Delta t\, \mathbf{A}) + \sum_{k}^{\prime} [\exp(\Delta t\, \omega_k) - f(\Delta t\, \omega_k)] U_k V_k^T \tag{11}$$

where the sum $\sum_{k}^{\prime}$ is over only those k for which equation (10) does not hold.

The vectors U_k and V_k are easily calculated from their defining equations as

$$\mathbf{U}_k = \mathrm{col}\left[1 \quad \frac{\mu_1}{\lambda_1 + \omega_k} \quad \cdots \quad \frac{\mu_G}{\lambda_G + \omega_k}\right]$$

where

$$\mu_1 = \frac{\beta_1}{\Lambda}, \ldots, \mu_G = \frac{\beta_G}{\Lambda}$$

and

$$\mathbf{V}_k = \nu_k\, \mathrm{col}\left[1 \quad \frac{\lambda_1}{(\lambda_1 + \omega_k)} \quad \cdots \quad \frac{\lambda_G}{(\lambda_G + \omega_k)}\right]$$

where ν_k is the normalization factor, given by

$$\nu_k = \left[1 + \sum_{i=1}^{G} \frac{\mu_i \lambda_i}{(\lambda_i + \omega_k)^2}\right]^{-1} \prec 1.$$

3. The Padé approximations and related inversions (rational matrix functions)

The accurate evaluation of the matrix exponential is itself a difficult problem. Unless the time step size is uncomfortably small, the power series defining the exponential converges too slowly for practical use. What is required here is to replace the exponential in equation (11) by certain rational matrix functions to approximate it. To achieve this a particular class of approximations for the exponential function, namely, the Padé rational approximations [12, 13], is considered. In addition to the four rational approximations mentioned in the previous work [1], we treated eight such Padé approximations of varying accuracy with time varying reactivity. For any of these approximations in which the degree of the polynomial's denominator is larger than unity, we have a full square matrix of order $(G + 1)$ to invert. This is a task one normally tries to avoid, particularly for the case of varying reactivity when such inversion needs to be done at every time step.

However, we have developed a new method [1] to obtain a simple analytical expression for such inverses by going temporarily to the complex plane. The appendix summarizes this technique briefly. As a result, the same number of arithmetic operations that are sufficient to multiply the inverse of a polynomial of the matrix $\mathbf{A}$ by a vector is equal to those required to multiply the polynomial by itself. This fact makes the computational effort involved in using implicit methods of any order equal to that used for explicit methods of the same order (Taylor series expansion). However, the instabilities associated with the latter are avoided. Table 1 shows different types of Padé approximations considered here together with the associated errors and the form of such inverses.

The inverse of $[\mathbf{I} - \varepsilon\mathbf{A}]$ required by the Padé approximations is to be found using the analytical inversion method (see the appendix) as

$$[\mathbf{I} - \varepsilon\mathbf{A}]^{-1} = \gamma^{-1}\mathbf{a}\mathbf{b}^T + \mathbf{C} \tag{12}$$

Table 1. Different types of rational approximation (Padé approximations) of the exponential matrix.

Case Padé	Explicit form	Implicit form	Errors	ε
1 $f_{0,1}$	$\dfrac{I}{[I-(\Delta t)A]}$	$[I-\varepsilon A]^{-1}$	$-\dfrac{(\Delta t)^2 A^2}{2}$ $+O(\Delta t)^3$	Δt
2 $f_{1,1}$	$\dfrac{\left(I+\frac{(\Delta t)A}{2}\right)}{\left(I-\frac{(\Delta t)A}{2}\right)}$	$[I-\varepsilon A]^{-1}\{I+\varepsilon A\}$	$-\dfrac{(\Delta t)^3 A^3}{12}$ $+O(\Delta t)^4$	$\dfrac{\Delta t}{2}$
3 $f_{2,1}$	$\dfrac{\left(I+\frac{2(\Delta t)A}{3}+\frac{(\Delta t)^2 A^2}{6}\right)}{\left(I-\frac{(\Delta t)A}{3}\right)}$	$[I-\varepsilon A]^{-1}\left\{I+\frac{2(\Delta t)A}{3}+\frac{(\Delta t)^2 A^2}{6}\right\}$	$-\dfrac{(\Delta t)^4 A^4}{72}$ $+O(\Delta t)^5$	$\dfrac{\Delta t}{3}$
4 $f_{3,1}$	$\dfrac{\left(I+\frac{3(\Delta t)A}{4}+\frac{(\Delta t)^2 A^2}{4}+\frac{(\Delta t)^3 A^3}{24}\right)}{\left(I-\frac{(\Delta t)A}{4}\right)}$	$[I-\varepsilon A]^{-1}\left\{I+\frac{3(\Delta t)A}{4}+\frac{(\Delta t)^2 A^2}{4}+\frac{(\Delta t)^3 A^3}{24}\right\}$	$-\dfrac{(\Delta t)^5 A^5}{480}$ $+O(\Delta t)^6$	$\dfrac{\Delta t}{4}$
5 $f_{0,2}$	$\dfrac{I}{\left(I-(\Delta t)A+\frac{(\Delta t)^2 A^2}{2}\right)}$	$[I-\varepsilon A]^{-1}[I-\bar\varepsilon A]^{-1}$	$+\dfrac{(\Delta t)^3 A^3}{6}$ $+O(\Delta t)^4$	$\dfrac{\Delta t}{2}(1+i)$
6 $f_{1,2}$	$\dfrac{\left(I+\frac{(\Delta t)A}{3}\right)}{\left(I-\frac{2(\Delta t)A}{3}+\frac{(\Delta t)^2 A^2}{6}\right)}$	$[I-\varepsilon A]^{-1}[I-\bar\varepsilon A]^{-1}\left\{I+\frac{(\Delta t)A}{3}\right\}$	$+\dfrac{(\Delta t)^4 A^4}{72}$ $+O(\Delta t)^5$	$\dfrac{\Delta t}{3}\left(1+\frac{i}{\sqrt{2}}\right)$
7 $f_{2,2}$	$\dfrac{\left(I+\frac{(\Delta t)A}{2}+\frac{(\Delta t)^2 A^2}{12}\right)}{\left(I-\frac{(\Delta t)A}{2}+\frac{(\Delta t)^2 A^2}{12}\right)}$	$[I-\varepsilon A]^{-1}[I-\bar\varepsilon A]^{-1}\left\{I+\frac{(\Delta t)A}{2}+\frac{(\Delta t)^2 A^2}{12}\right\}$	$+\dfrac{(\Delta t)^5 A^5}{720}$ $+O(\Delta t)^6$	$\dfrac{\Delta t}{4}\left(1+\frac{i}{\sqrt{12}}\right)$
8 $f_{3,2}$	$\dfrac{\left(I+\frac{3(\Delta t)A}{5}+\frac{3(\Delta t)^2 A^2}{20}+\frac{(\Delta t)^3 A^3}{60}\right)}{\left(I-\frac{2(\Delta t)A}{5}+\frac{(\Delta t)^2 A^2}{20}\right)}$	$[I-\varepsilon A]^{-1}[I-\bar\varepsilon A]^{-1}$ $\left\{I+\frac{3(\Delta t)A}{5}+\frac{3(\Delta t)^2 A^2}{20}+\frac{(\Delta t)^3 A^3}{60}\right\}$	$+\dfrac{(\Delta t)^6 A^6}{7200}$ $+O(\Delta t)^7$	$\dfrac{\Delta t}{5}\left(1+\frac{i}{2}\right)$
9 $f_{0,3}$	$\dfrac{I}{\left(I-(\Delta t)A+\frac{(\Delta t)^2 A^2}{2}-\frac{(\Delta t)^3 A^3}{6}\right)}$	$[I-\varepsilon A]^{-1}[I-\bar\varepsilon A]^{-1}[I-eA]^{-1}$	$-\dfrac{(\Delta t)^4 A^4}{24}$ $+O(\Delta t)^5$	$\Delta t(0.1867,0.4808)$ $e=\Delta t(0.6265)$
10 $f_{1,3}$	$\dfrac{\left(I+\frac{(\Delta t)A}{4}\right)}{\left(I-\frac{3\Delta t A}{4}+\frac{(\Delta t)^2 A^2}{4}-\frac{(\Delta t)^3 A^3}{24}\right)}$	$[I-\varepsilon A]^{-1}[I-\bar\varepsilon A]^{-1}[I-eA]^{-1}\left\{I+\frac{(\Delta t)A}{4}\right\}$	$-\dfrac{(\Delta t)^5 A^5}{480}$ $+O(\Delta t)^6$	$\Delta t(0.1846,0.2745)$ $e=\Delta t(0.3808)$
11 $f_{2,3}$	$\dfrac{\left(I+\frac{2(\Delta t)A}{5}+\frac{(\Delta t)^2 A^2}{20}\right)}{\left(I-\frac{3\Delta t A}{5}+\frac{3(\Delta t)^2 A^2}{20}-\frac{(\Delta t)^3 A^3}{60}\right)}$	$[I-\varepsilon A]^{-1}[I-\bar\varepsilon A]^{-1}[I-eA]^{-1}$ $\left\{I+\frac{2(\Delta t)A}{5}+\frac{(\Delta t)^2 A^2}{20}\right\}$	$-\dfrac{(\Delta t)^6 A^6}{7200}$ $+O(\Delta t)^7$	$\Delta t(0.6256,0.1849)$ $e=\Delta t(0.2749)$
12 $f_{3,3}$	$\dfrac{\left(I+\frac{(\Delta t)A}{2}+\frac{(\Delta t)^2 A^2}{10}+\frac{(\Delta t)^3 A^3}{120}\right)}{\left(I-\frac{\Delta t A}{2}+\frac{(\Delta t)^2 A^2}{10}-\frac{(\Delta t)^3 A^3}{120}\right)}$	$[I-\varepsilon A]^{-1}[I-\bar\varepsilon A]^{-1}[I-eA]^{-1}$ $\left\{I+\frac{(\Delta t)A}{2}+\frac{(\Delta t)^2 A^2}{10}+\frac{(\Delta t)^3 A^3}{120}\right\}$	$-\dfrac{(\Delta t)^7 A^7}{100\,800}$ $+O(\Delta t)^8$	$\Delta t(0.1424,0.1358)$ $e=\Delta t(0.2153)$

where ε is a scalar. The validity of this expression can be verified directly by multiplying equation (12) by $[\mathbf{I}-\varepsilon\mathbf{A}]$. For a complex conjugate pair, a pair of factors was considered:

$$[\mathbf{I}-\varepsilon\mathbf{A}]^{-1}[\mathbf{I}-\bar\varepsilon\mathbf{A}]^{-1}=[\mathbf{I}-2\,\mathrm{Re}(\varepsilon)\mathbf{A}+|\varepsilon|^2\mathbf{A}^2]^{-1}.$$

This is a real matrix and has a real inverse (for more details see the appendix).

4. Numerical results

The general solution for $N(t)$ has been coded in Visual FORTRAN and developed to include other types of Padé approximations. The designated AIM (analytical inversion method) code, figure 1, is applied to the step reactivity insertion, ramp input and oscillatory reactivity changes. Whenever the reactivity is given, including the case in which the feedback reactivity is a function of neutron density, the developed code can provide a straightforward procedure for computing the neutron density. The values for Λ, β_i and λ_i (in s^{-1}) for the representative reactors are shown in table 2, for six delayed neutron groups.
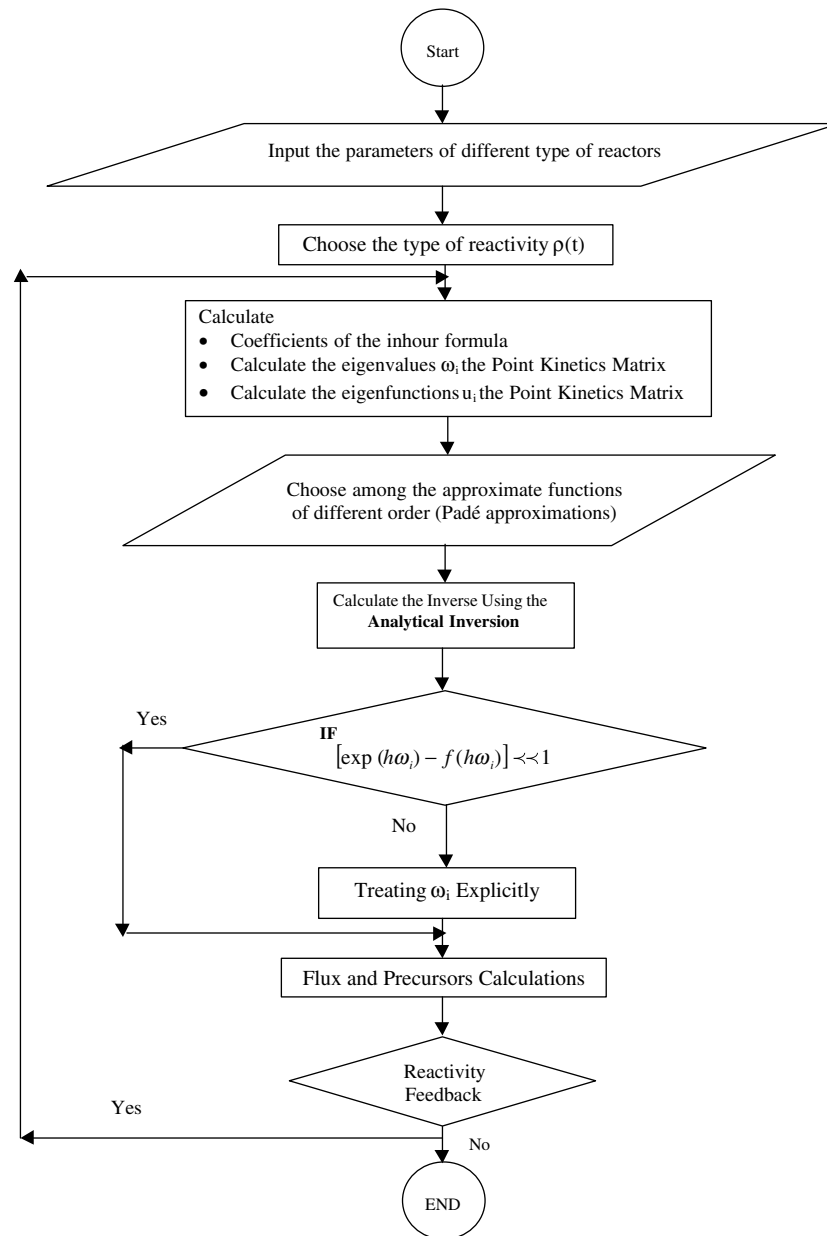
Figure 1. Block diagram for AIM.

4.1. Step reactivity

Tables 3 and 4 show four different transients, all starting from equilibrium condition and with $N(0) = 1$ for two representative thermal and fast reactors. These tables present the exact $N(t)$ [1] and the relative per cent errors of the calculations for several options of the method presented in this work. The results are shown for selected times t during the transient and for several values of the time step size used in the calculations. The results in table 3 indicate the RPEs (relative percentage errors) for the considered Padé approximations of a thermal reactor

Table 2. Delayed neutron parameters of typical reactors.

Neutron group	Thermal reactor		Fast reactor		^{235}U–graphite reactor	
	λ_i	β_i	λ_i	β_i	λ_i	β_i
1	0.0127	2.850E−04	0.0129	1.672E−04	0.0124	2.10E−04
2	0.0317	1.597E−03	0.0311	1.232E−03	0.0305	1.41E−03
3	0.0115	1.410E−03	0.134	9.504E−04	0.111	1.27E−03
4	0.311	3.052E−03	0.331	1.443E−03	0.301	2.55E−03
5	1.40	9.600E−04	1.260	4.534E−04	1.13	7.40E−04
6	3.87	1.950E−04	3.210	1.540E−04	3.0	2.70E−04
	$\beta_{tot} = 0.0075$		$\beta_{tot} = 0.0044$		$\beta_{tot} = 0.00645$	
	$\Lambda = 5.0 \times 10^{-4}$ s		$\Lambda = 1.0 \times 10^{-7}$ s		$\Lambda = 1.0 \times 10^{-4}$ s	
					$\Lambda = 1.0 \times 10^{-5}$ s	

at +0.5\$ for the explicitly treated and untreated most effective roots. On the other hand, table 4 represents the RPEs of a fast reactor at +0.5\$.

The values of the explicitly treated term $[\exp(\Delta t \, \omega_i) - f(\Delta t \, \omega_i)]$ for both thermal and fast reactors are presented in table 5. Spotlight on this table shows that the most effective dominant roots are ω_5 and ω_6 terms for negative reactivity within the interval $(-1\$, 0\$)$. While in the case of positive reactivity the most effective roots are ω_0, ω_5 and ω_6 terms, which have a large magnitude within the reactivity interval $(0\$, +1\$)$. At low-order Padé approximations, the most effective terms are ω_5 and ω_6 within the reactivity interval $(-3/4\$, 3/4\$)$ for a fast reactor. The effect of these terms decreases at higher order of Padé approximations, while the effect of ω_0 term increases.

The above considerations, coupled with the fact that for most practical cases only one of the ω_0 and ω_i ($i = 5$, 6) is of a large magnitude, indicate that in many problems satisfactory results will be obtained by treating explicitly only three terms in equation (11). Comparison of the RPEs for treated and untreated roots in tables 3 and 4 confirms that a large correction effect could be obtained by treating the most dominant roots explicitly, a feature shared by most considered cases at different time steps.

4.2. Ramp reactivity input

To check the accuracy of the new adopted technique comparisons were made to the few special cases for which analytic solutions exist. Two such cases are presented here, and the results are typical for the other studied cases.

The first example of a ramp reactivity input at a slow rate of $0.1\$ \, \text{s}^{-1}$ is treated by Nishigori [14] and Chao [4] where the parameters for six delayed neutron groups are taken from the latter. The generation time, $\Lambda = 2 \times 10^{-5}$ s, is kept constant. The values of $N(t)$ obtained with the AIM are compared to those obtained with the θ-weighting method reported by Porsching [15], the SCM method of Chao [4] and the analytical solution of Nishigori [14], table 6. Data in this table show that the AIM results are as good as or consistent with those of θ-weighting and SCM even though AIM uses time steps much larger than those of the other methods.

The second example is taken from the work reported by Keepin and Cox [10]. The $N(t)$ response to linear time variation of reactivity $\rho(t) = a\,t$ from initial equilibrium for assumed values of the prompt neutron generation times, $\Lambda = 10^{-5}$ and 10^{-4} s, is shown in figure 2. It is clear that the neutron density profile agrees within graph-reading error with the numerical results presented by Keepin and Cox [10].

Table 3. The RPEs and exact $N(t)$ for different cases of Padé approximations for a thermal reactor at +0.5$.

		Time (s)							
		0.1		1.0		5.0		10	
Δt	Case	Automatic inclusion of ω_i terms	Without inclusion of ω_i terms	Automatic inclusion of ω_i terms	Without Inclusion of ω_i terms	Automatic inclusion of ω_i terms	Without inclusion of ω_i terms	Automatic inclusion of ω_i terms	Without inclusion of ω_i terms
0.1	1	1.1890E−04	−5.8749E+00	8.7007E−05	−1.0758E−01	3.4352E−05	7.8549E−01	2.2540E−06	1.5391E+00
	2	−3.8168E−05	1.2025E+00	1.4849E−05	9.9404E−03	2.4580E−06	2.3863E−03	−2.4355E−05	4.3443E−03
	3	−2.2772E−05	−2.0304E−01	1.1264E−05	−9.0382E−04	−7.4225E−06	2.1045E−06	−4.1799E−05	−2.1629E−05
	4	−2.2688E−05	2.8755E−02	1.8375E−05	1.1665E−04	7.0246E−06	6.7927E−06	−1.8538E−05	−1.8781E−05
	5	−1.2045E−05	−1.2579E+0	5.5281E−07	−1.7138E−02	−4.7668E−05	−4.8666E−06	−1.1718E−04	−8.9719E−03
	6	−2.5386E−05	1.3059E−01	1.3733E−05	6.3715E−04	−3.6772E−06	−5.7199E−03	−3.6460E−05	−4.2936E−05
	7	−2.3764E−05	−1.3652E−02	1.3916E−05	−3.4530E−05	−1.9152E−07	−9.8213E−08	−2.8959E−05	−2.8859E−05
	8	−2.3175E−05	1.2997E−03	1.6874E−05	2.2015E−05	3.8571E−06	7.3461E−06	−2.3705E−05	−1.7122E−05
	9	−6.5432E−05	−2.4073E−01	1.3805E−05	−1.3628E−03	8.2864E−06	2.4137E−05	−1.2478E−05	2.5877E−05
	10	−2.8350E−05	1.4262E−02	1.4732E−06	5.4645E−05	3.2086E−05	−3.0390E−05	−8.4248E−05	−8.0996E−05
	11	−2.5680E−05	−1.0147E−03	1.7548E−05	1.5351E−05	3.9025E−06	7.4001E−06	−2.4605E−05	−1.8028E−05
	12	−1.6628E−05	5.2385E−05	2.0204E−05	2.0413E−05	1.2072E−05	1.2701E−05	−9.3569E−06	−9.3578E−06
0.25	1			1.1302E−04	−4.1137E−01	4.5230E−05	2.0105E+00	4.2675E−05	3.9631E+00
	2			−2.2549E−05	5.1283E−02	−5.0988E−05	1.4859E−02	−9.8958E−05	2.7223E−02
	3			5.1146E−08	−4.4760E−02	−1.8927E−05	7.0043E−05	−5.3221E−05	1.5702E−04
	4			2.4814E−05	5.1024E−03	1.1427E−05	4.0417E−06	−1.7088E−05	−2.5012E−05
	5			7.9307E−05	−9.5790E−02	8.0555E−05	−3.0483E−02	7.4821E−05	−5.6313E−02
	6			1.8185 E−05	7.6659E−03	5.3043E−06	−7.1852E−05	−2.2008E−05	−2.1411E−04
	7			1.7698 E−05	−2.4788E−03	9.0535E−06	1.0250E−05	−1.3127E−05	−1.1676E−05
	8			5.5064E−06	5.7145E−04	−2.0511E−05	−1.8583E−05	−6.3691E−05	−5.9343E−05
	9			2.5591E−05	−1.3838E−02	3.1507E−05	2.7885E−04	2.1502E−05	6.1862E−04
	10			9.2970E−06	1.4794E−03	−1.6024E−05	−1.5363E−05	−5.8344E−05	−5.7935E−05
	11			1.7693E−06	−2.9853E−04	−2.7897E−05	−2.4698E−05	−7.5693E−05	−6.9979E−05
	12			2.2280E−05	8.0880E−05	1.2712E−05	1.2614E−05	−1.0245E−05	−1.0345E−05
0.5	1			3.1144E−05	−1.2038E+00	−4.1621E−05	4.1883E+00	−1.4861E−05	8.3418E+00
	2			−9.9101E−05	−3.7411E+00	−8.9777E−05	5.9091E−02	−1.1604E−04	1.0930E−01
	3			−8.0823E−06	−7.2275E+00	−3.0822E−05	−9.1207E−03	−5.3746E−05	1.5206E−03
	4			9.4930E−05	−5.3327E+00	8.9155E−05	−2.2499E−03	5.2561E−05	−3.0656E−05
	5			7.3511E−05	−3.5714E−01	1.7928E−04	−1.2547E−01	−3.7236E−05	−2.3266E−01
	6			−1.3669E−05	−7.9163E−02	−3.6223E−05	−6.7459E−04	−7.8128E−05	−1.6524E−03
	7			−1.0839E−05	−2.0426E−01	−4.4836E−05	−5.3865E−05	−9.5190E−05	−1.0012E−04
	8			1.7566E−05	−2.5455E−02	−3.2008E−06	−1.2144E−05	−4.2018E−05	−4.9320E−05
	9			5.2806E−05	−7.2427E−02	6.9508E−05	2.2633E−03	7.3503E−05	5.0633E−03
	10			1.7437E−06	1.0035E−02	−2.1887E−05	4.2929E−06	−6.2586E−05	−3.8857E−05
	11			−2.7505E−06	−1.6636E−02	−3.2409E−05	−2.7653E−05	−7.9895E−05	−7.2029E−05
	12			7.5848E−06	4.6418E−03	−1.9300E−05	−2.1176E−05	−6.2925E−05	−6.4840E−05
1.0	1			−8.3448E−05	−3.0368E+0	−1.6363E−04	9.1453E+0	−5.5655E−05	1.8634E+1
	2			−7.2758E−04	2.0266E+1	−2.3551E−04	1.4425E+0	−2.5944E−04	3.9540E−1
	3			9.6389E−04	−5.9450E+1	2.6236E−05	−3.4555E+2	2.6735E−06	−3.6468E+3
	4			−1.2144E−03	1.2572E+2	7.5065E−04	1.5604E+4	7.3340E−04	−7.4367E+6
	5			3.1173E−05	−1.3003E+0	−8.2029E−05	−5.3094E−01	−1.4369E−04	−9.8862E−01
	6			−1.5904E−04	3.2429E+0	−9.0478E−05	−5.4745E−03	−1.3359E−04	−1.3167E−02
	7			1.2567E−04	−7.6058E+0	−1.8299E−05	−1.2129E−02	−6.4767E−05	−3.0299E−04
	8			−1.1510E−04	1.3303E+1	5.9622E−05	2.0665E−01	2.1423E−05	−1.3586E−03
	9			6.1222E−05	−3.5425E−01	7.3221E−05	2.0295E−02	1.0506E−04	4.3177E−02
	10			−3.6513E−05	7.3741E−01	−3.5427E−05	3.3681E−04	−7.3264E−05	2.9874E−04
	11			2.3954E−05	−1.3750E+0	−1.3469E−05	−2.9667E−05	−5.0063E−05	−4.3784E−05
	12			−1.5658E−05	1.9837E+0	−1.4419E−05	−9.7770E−06	−6.1372E−05	−7.3433E−05
Exact $N(t)$		1.533 113		2.511 494		5.753 393		14.215 03	

4.3. Oscillatory reactivity

In this case the reactivity $\rho(t)$ is a function of time given as

$$\rho(t) = \rho_0 + \mu \sin \omega t = \rho_0 + \frac{1}{2}\mu \left[\frac{e^{i\omega t}}{i} + \text{C.C.} \right]$$

Table 4. The RPEs and exact $N(t)$ for different cases of Padé approximations for a fast reactor at +0.5$.

		Time (s)							
		0.1		1.0		5.0		10	
Δt	Case	Automatic inclusion of ω_i terms	Without inclusion of ω_i terms	Automatic inclusion of ω_i terms	Without inclusion of ω_i terms	Automatic inclusion of ω_i terms	Without inclusion of ω_i terms	Automatic inclusion of ω_i terms	Without inclusion of ω_i terms
0.1	1	2.8605E−05	−1.0359E−01	2.1641E−05	−3.3818E−03	5.2860E−05	6.2100E−01	8.2686E−05	1.2193E+0
	2	−7.4251E−06	4.8099E+1	−2.0117E−05	−3.6967E+1	−2.6773E−05	−1.6183E+1	−4.2525E−05	−6.5374E+0
	3	9.8225E−04	−5.2833E+4	4.4541E−04	−9.463E+31	4.3617E−04	−1.778E+153	4.2635E−04	−7.892E+304
	4	1.2253E+00	3.8693E+7	−2.7887E−01	−4.200E+60	−2.8126E−01	−3.063E+296	−2.7854E−01	−8.123E+350
	5	9.9310E−06	−7.3383E−03	−5.9929E−06	−7.3331E−03	−4.2950E−06	−3.4799E−03	−1.0013E−05	−6.2875E−03
	6	1.1745E−05	4.3862E−02	−3.5766E−06	1.1888E−04	4.3435E−07	6.5060E−07	−2.5022E−06	−4.4618E−06
	7	−6.8318E−05	−4.7919E+1	−2.3747E−05	−3.5652E+1	−5.1711E−06	−1.3495E+1	−4.8368E−07	−4.5476E+0
	8	4.9301E−03	3.5062E+4	−8.6401E−03	−1.568E+30	−7.0450E−03	−2.222E+144	−6.6062E−03	−1.232E+287
	9	2.5054E−05	−4.5973E−04	1.4114E−05	−3.0354E−04	3.5701E−05	4.4876E−05	5.2512E−05	7.6355E−05
	10	8.8884E−06	7.6354E−05	−7.4402E−06	−2.5518E−06	−6.8366E−06	−5.2296E−06	−1.3873E−05	−1.0868E−05
	11	3.7753E−05	−6.5156E−02	9.2965E−06	1.0086E−05	3.8666E−07	3.5651E−06	−1.2968E−05	−7.0645E−06
	12	−2.2098E−02	4.7637E+1	−1.4045E−02	−3.3758E+1	−1.0308E−02	−1.0276E+1	−9.6113E−03	−2.6394E+0
0.25	1			3.4271E−06	1.1750E−02	1.3654E−05	1.5848E+00	1.8433E−05	3.1255E+00
	2			−1.6205E−05	−3.7514E+1	−2.0751E−05	−1.7459E+1	−3.3956E−05	−7.6003E+0
	3			1.0302E−03	−2.1426E+15	1.0383E−03	−1.0580E+70	1.0339E−03	−2.795E+138
	4			−1.9999E+0	−2.4156E+28	−7.8337E−01	−1.927E+135	−5.5366E−01	−9.272E+268
	5			2.8692E−05	−3.9312E−02	6.7428E−05	−2.1934E−02	1.0615E−04	−3.9798E−02
	6			−2.2770E−05	1.7398E−03	−3.5016E−05	−7.9822E−05	−5.7468E−05	−1.7665E−04
	7			1.1780E−04	−3.7322E+1	8.9855E−05	−1.6968E+1	7.2573E−05	−7.1877E+0
	8			−2.5809E−01	−4.201E+14	−1.9681E−01	−3.068E+66	−1.8345E−01	−2.3507E31
	9			−1.7675E−05	−3.7703E−03	−1.5143E−05	1.3754E−04	−2.2692E−05	3.5697E−04
	10			−7.9301E−06	1.4147E−04	−1.7671E−05	−1.6668E−05	−3.7167E−05	−3.6432E−05
	11			−1.1483E−04	−1.2253E−04	−8.1336E−05	−7.8832E−05	−7.8890E−05	−7.4165E−05
	12			7.5635E−02	−3.7008E+1	5.4691E−02	−1.6238E+1	5.0860E−02	−6.5719E+0
0.5	1			1.3584E−05	9.0896E−02	3.5985E−05	3.2844E+0	5.5467E−05	6.5273E+0
	2			2.6526E−07	−3.7515E+0	6.8001E−06	−1.7618E+1	7.0113E−06	−7.7101E+0
	3			7.9180E−04	−1.1375E+0	1.2132E−03	−4.462E+38	1.2772E−03	−4.972E+75
	4			−1.1673E+2	−1.5286E+16	−1.8571E+3	−1.955E+74	−4.7659E+4	−9.549E+146
	5			−2.8583E−05	−1.2943E−01	−5.2032E−05	−9.0086E−02	−8.7850E−05	−1.6423E−01
	6			−2.8919E−05	1.2989E−02	−4.6429E−05	−4.3575E−04	−7.5264E−05	−1.0728E−03
	7			−8.4294E−04	−3.7573E+0	−5.3938E−04	−1.7541E+1	−4.9668E−04	−7.6843E+0
	8			−1.7408E+0	−5.046E+08	−1.2968E+0	−7.669E+36	−1.2076E+0	−1.468E+72
	9			−7.5681E−06	−2.0136E−02	4.8677E−06	1.3381E−03	7.2863E−06	3.1414E−03
	10			8.0354E−06	1.9479E−04	2.0768E−05	3.5948E−05	2.8345E−05	4.0248E−05
	11			−2.9777E−04	−5.5383E−04	−2.0997E−04	−2.0778E−04	−1.9937E−04	−1.9456E−04
	12			−5.6444E−01	−3.7430E+1	−3.9935E−01	−1.7399E+1	−3.7113E−01	−7.6390E+0
1.0	1			−1.8144E−05	4.3318E−01	−3.2788E−05	7.0860E+0	−5.7620E−05	1.4319E+01
	2			1.2542E−05	3.8330E+1	2.1408E−05	1.7882E+1	2.8958E−05	−7.5185E+0
	3			6.0594E−03	−4.1403E+5	5.4382E−03	−2.850E+21	5.3393E−03	−2.028E+41
	4			1.5544E+2	3.0359E+9	2.2185E+04	6.0426E+40	−1.2418E+7	−9.116E+79
	5			−1.3184E−05	−3.9077E−01	−2.0552E−05	−3.7800E−01	−3.6952E−05	−6.9341E−01
	6			−2.0098E−05	1.1682E−01	−3.1979E−05	−3.3508E−03	−5.3320E−05	−8.2473E−03
	7			−4.7791E−03	−3.7686E+1	−1.0979E−03	−1.7688E+1	−1.0135E−03	−7.8137E+0
	8			8.3473E+00	2.7590E+5	−2.8803E+0	3.746E+20	−2.7655E+0	−3.5041E+39
	9			−8.0036E−06	−8.6646E−02	3.3106E−05	1.2214E−02	6.7952E−05	2.6762E−02
	10			−9.6575E−06	2.4867E−02	−1.4272E−05	2.0839E−04	−2.7692E−05	1.6851E−04
	11			−1.3104E−03	−1.4989E−02	−8.5155E−04	−8.5887E−04	−7.8250E−04	−7.7590E−04
	12			−1.3735E+1	2.3875E+1	−8.9880E+0	49.3844E+0	−8.3345E+0	−1.0735E+1
Exact $N(t)$		2.075 317		2.655 853		5.641 100		12.746 54	

where ρ_0 is the constant part of the excess reactivity, $\sin \omega t$ is a given function characterizing the time dependence of the reactivity and C.C. is the a complex conjugate of the first term. The parameter μ is a positive number that represents the magnitude of the variable part of the excess reactivity in dollars. It will be assumed that this parameter is sufficiently small compared to unity. This is a real assumption since, except in the accidental case, the excess

Table 5. Values of the coefficients $|\exp(h\omega_i) - f(h\omega_i)|$ for different cases of Padé approximations ω_i, $i = 1, 2, 3, 4$, ω_0, ω_5, ω_6 are the real roots of the inhour equation (1$ \equiv$ 1 dollar reactivity)

Type	Reactivity	ω	Case 1 $\exp(h\omega_i) - f_1(h\omega_i)$		Case 2 $\exp(h\omega_i) - f_2(h\omega_i)$		Case 3 $\exp(h\omega_i) - f_3(h\omega_i)$		Case 4 $\exp(h\omega_i) - f_4(h\omega_i)$	
			min	max	min	max	min	max	min	max
Thermal reactor	$-1\$ \to 0\$$	ω_0	0.0	7.224 40E−05	0.0	1.229 99E−07	0.0	1.612 35E−10	0.0	5.482 89E−13
		ω_i	1.288 06E−06	1.632 01E−01	2.833 17E−10	6.150 01E−02	5.590 54E−11	1.749 35E−02	3.735 08E−17	4.035 86E−03
		ω_5	4.005 26E−02	1.869 18E−01	3.088 29E−03	3.342 57E−01	2.116 31E−04	3.666 16E−01	1.256 30E−05	2.967 68E−01
		ω_6	3.202 22E−02	2.033 16E−01	8.521 84E−02	8.758 86E−01	2.963 13E−02	1.202 04E+1	8.251 78E−03	1.103 32E+2
	$0\$ \to 1\$$	ω_0	0.0	8.680 86E+0	0.0	9.915 67E+01	0.0	1.879 42E+0	0.0	3.223 86E−01
		ω_i	8.584 31E−07	1.559 83E−01	1.878 35E−10	1.668 58E−02	4.877 32E−11	1.413 29E−02	3.735 08E−17	1.799 62E−3
		ω_5	2.085 84E−02	2.036 07E−01	9.953 73E−04	3.289 08E−01	4.367 79E−05	3.524 75E−01	1.680 70E−06	2.797 39E−01
		ω_6	5.019 70E−02	2.020 92E−01	4.655 95E−03	7.710 94E−01	3.779 92E−04	4.967 94E+0	2.643 53E−05	2.159 46E+1
Fast reactor	$-3/4\$ \to 0\$$	ω_0	0.0	7.115 19E−05	0.0	1.440 29E−07	0.0	1.604 31E−10	0.0	5.275 36E−13
		ω_i	1.090 97E−06	1.524 04E−01	2.691 84E−10	5.030 69E−02	5.496 42E−11	1.273 74E−02	1.734 72E−17	2.634 02E−03
		ω_5	3.006 05E−02	1.987 10E−01	1.861 19E−03	2.661 43E−01	1.041 28E−04	2.272 53E−01	5.076 78E−06	1.458 87E−01
		ω_6	1.298 68E−05	2.272 19E−04	9.990 91E−01	9.999 48E−01	2.196 52E+3	3.849 66E+4	3.219 40E+6	9.880 44E+8
	$0\$ \to 3/4 \$$	ω_0	0.0	1.544 67E−02	0.0	5.906 13E−02	0.0	5.369 68E−03	0.0	4.917 29E−04
		ω_i	8.969 81E−07	1.478 42E−01	2.006 37E−10	4.624 92E−02	4.941 86E−11	1.116 89E−02	4.147 07E−17	2.209 05E−03
		ω_5	2.718 53E−02	2.011 98E−01	1.563 87E−03	2.618 07E−01	8.171 39E−05	2.198 65E−01	3.727 69E−06	1.389 89E−01
		ω_6	2.272 66E−05	9.081 37E−04	9.963 71E−01	9.999 09E−01	5.465 90E+2	2.199 67E+4	1.998 99E+5	3.225 99E+8

Table 5. (Continued.)

Type	Reactivity	ω	Case 5 $\exp(h\omega_i) - f_5(h\omega_i)$		Case 6 $\exp(h\omega_i) - f_6(h\omega_i)$		Case 7 $\exp(h\omega_i) - f_7(h\omega_i)$		Case 8 $\exp(h\omega_i) - f_8(h\omega_i)$	
			min	max	min	max	min	max	min	max
Thermal reactor	$-1 \rightarrow 0\$$	ω_0	0.0	2.920 81E−07	0.0	6.540 59E−10	0.0	3.665 35E−13	0.0	1.695 55E−10
		ω_i	5.659 95E−10	4.588 94E−02	5.601 41E−11	8.965 19E−03	7.367 15E−17	1.602 93E−03	5.594 81E−11	1.839 93E-4
		ω_5	4.615 30E−03	6.131 61E−02	1.734 38E−04	6.756 92E−02	7.176 88E−06	5.210 48E−02	2.959 56E−07	3.168 07E−02
		ω_6	2.048 74E−03	6.898 85E−02	1.359 75E−02	9.829 91E−02	3.006 16E−03	6.723 58E−01	5.857 62E−04	5.791 66E+0
	$0\$ \rightarrow 1\$$	ω_0	0.0	6.766 47E+0	0.0	2.683 92E+0	0.0	4.549 65E−01	0.0	6.638 65E−02
		ω_i	3.753 00E−10	4.248 16E−02	4.883 43E−11	7.536 24E−03	5.421 01E−17	1.240 58E−03	4.879 25E−11	1.839 93E−04
		ω_5	1.644 62E−03	6.879 45E−02	3.830 25E−05	6.638 35E−02	1.011 52E−06	4.998 99E−02	3.308 01E−08	2.974 92E−02
		ω_6	6.621 64E−03	6.863 15E−02	2.996 69E−04	9.829 91E−02	1.472 03E−05	4.606 71E−01	7.042 69E−07	1.780 74E+0
Fast reactor	$-3/4\$ \rightarrow 0\$$	ω_0	0.0	2.854 63E−07	0.0	6.423 88E−10	0.0	3.526 49E−13	0.0	3.557 56E−10
		ω_i	5.377 69E−10	4.084 04E−02	5.506 44E−11	6.918 28E−03	4.147 07E−17	1.094 61E−03	5.500 28E−11	1.564 69E−04
		ω_5	2.925 82E−03	6.718 12E−02	8.828 65E−05	5.336 80E−02	2.977 23E−06	3.118 54E−02	1.056 92E−07	1.475 16E−02
		ω_6	3.373 14E−10	1.032 57E−07	2.597 16E−05	4.538 19E−04	9.972 77E−01	9.998 44E−01	1.461 03E+3	2.566 11E+4
	$0\$ \rightarrow 3/4\$$	ω_0	0.0	1.671 86E−01	0.0	7.654 55E−03	0.0	4.380 79E−04	0.0	2.659 62E−05
		ω_i	4.008 71E−10	3.879 40E−02	4.991 66E−11	6.203 96E−03	4.147 07E−17	9.341 55E−04	4.987 54E−11	1.275 17E−04
		ω_5	2.495 88E−03	6.828 03E−02	6.999 29E−05	5.242 34E−02	2.203 31E−06	3.007 76E−02	7.532 07E−08	1.399 35E−02
		ω_6	1.032 99E−09	1.649 42E−06	4.544 69E−05	1.806 39E−03	9.891 52E−01	9.997 27E−01	3.610 98E+2	1.466 11E+4

Table 5. (Continued.)

| Type	Reactivity	ω	Case 9 $\exp(h\omega_i) - f_9(h\omega_i)$		Case 10 $\exp(h\omega_i) - f_{10}(h\omega_i)$		Case 11 $\exp(h\omega_i) - f_{11}(h\omega_i)$		Case 12 $\exp(h\omega_i) - f_{12}(h\omega_i)$	
			min	max	min	max	min	max	min	max
Thermal reactor	$-1\$ \to 0\$$	ω_0	0.0	8.860 69E−10	0.0	2.156 85E−11	0.0	1.195 91E−10	0.0	1.154 01E−15
		ω_i	2.130 14E−13	1.847 34E−02	1.183 61E−15	1.183 06E−03	5.197 15E−11	1.147 02E−04	3.135 08E−17	1.105 63E−05
		ω_5	4.222 26E−04	2.207 71E−02	9.196 97E−06	1.133 03E−02	2.119 54E−07	9.198 68E−03	7.182 41E−09	4.182 72E−03
		ω_6	1.964 01E−04	2.112 24E−02	2.152 54E−03	1.121 47E−02	3.179 10E−04	6.182 91E−02	4.117 21E−05	4.128 61E−01
	$0\$ \to 1\$$	ω_0	0.0	1.136 48E+1	0.0	1.187 62E+0	0.0	1.144 97E−01	0.0	1.142 44E−02
		ω_i	1.130 55E−13	1.102 12E−02	7.107 56E−16	1.108 21E−03	4.181 06E−11	1.113 45E−04	3.135 08E−17	1.198 68E−05
		ω_5	1.102 93E−04	2.167 67E−02	1.170 65E−06	1.198 14E−02	1.149 72E−08	9.173 16E−03	4.148 27E−10	4.192 24E−03
		ω_6	7.132 61E−04	2.194 81E−02	1.136 16E−05	2.142 37E−02	5.161 08E−07	6.182 91E−02	2.112 27E−08	2.150 71E−01
Fast reactor	$-3/4\$ \to 0\$$	ω_0	0.0	8.193 61E−10	0.0	2.131 17E−11	0.0	3.138 31E−10	0.0	1.132 54E−15
		ω_i	1.186 89E−13	1.135 28E−02	1.127 12E−15	9.135 83E−04	5.102 58E−11	1.145 08E−04	4.147 07E−17	1.177 40E−05
		ω_5	2.130 21E−04	2.103 54E−02	3.122 45E−06	1.183 18E−02	7.174 52E−08	5.142 98E−03	2.138 94E−09	1.191 58E−03
		ω_6	1.114 19E−14	7.138 59E−11	1.111 84E−09	3.192 08E−07	3.195 23E−05	6.191 83E−04	9.145 60E−01	9.196 88E−01
	$0\$ \to 3/4\$$	ω_0	0.0	3.195 10E−02	0.0	8.195 61E−04	0.0	3.173 61E−05	0.0	1.167 23E−06
		ω_i	1.143 95E−13	9.146 69E−03	9.104 62E−16	8.145 84E−04	4.189 43E−11	8.148 87E−05	3.149 61E−17	8.108 87E−06
		ω_5	1.187 56E−04	2.115 11E−02	2.127 29E−06	1.183 18E−02	5.156 98E−08	5.127 92E−03	1.125 57E−09	1.184 09E−03
		ω_6	7.142 91E−14	4.193 70E−09	3.198 41E−09	4.112 39E−06	6.115 49E−05	2.185 06E−03	9.184 21E−01	9.194 55E−01
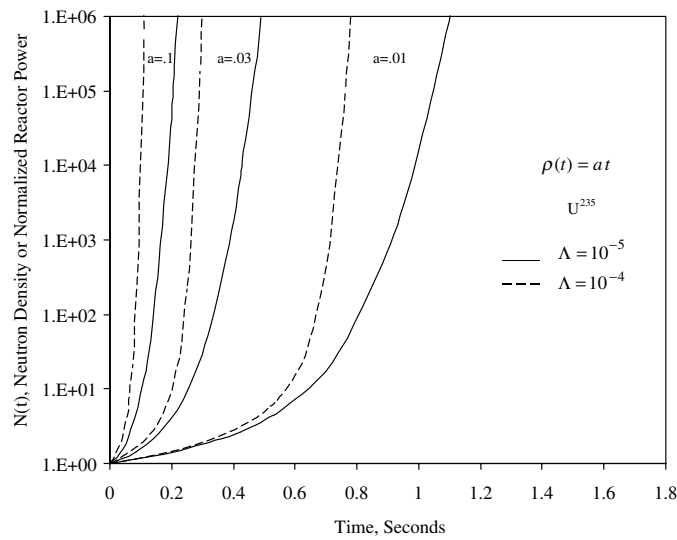
Figure 2. Response to linear variation of reactivity in U^{235} systems characterized by prompt neutron generation times in the range 10^{-4} s to 10^{-5} s.
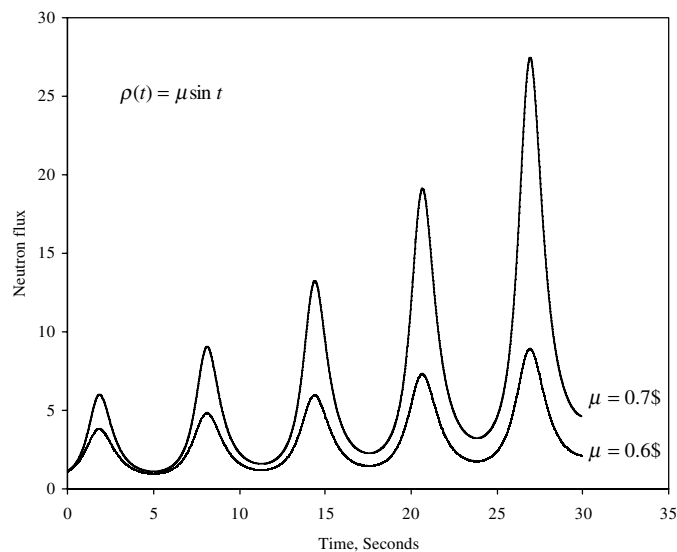

Figure 3. Variation of the flux with time for a sinusoidal reactivity input.

reactivity is always less than one dollar. The wave form oscillations of the flux is such that a modified sinusoidal curve is obtained for different values of the μ parameter (figure 3).

4.4. Compensated reactivity

The integration over t' in equation (5) may be evaluated using either a trapezoidal rule or Simpson's rule for numerical integration. The implicit assumption that the integrand can be

Table 6. Comparison of the AIM versus other methods for the 0.1 s^{-1} ramp reactivity (moderately fast ramp).

	θ-weighting [15]		SCM [4]	Nishegor [14]		AIM	
Time (s)	$\Delta t = 0.0001$ s	$\Delta t = 0.1$ s	$\Delta t = 0.1$ s	$\Delta t = 0.0005$ s	$\Delta t = 0.5$ s	$\Delta t = 0.001$ s	$\Delta t = 0.1$ s
2	1.3382	1.3383	1.3382	1.3382	1.3382	1.3382	1.3305
4	2.2283	2.2290	2.2284	Not available	Not available	2.2284	2.2117
6	5.5815	5.5885	5.5819	5.5821	5.5821	5.5820	5.5229
8	4.2781E+01[a]	4.3215E+01	4.2788E+01	Not available	Not available	4.2786E+01	4.2049E+01
9	4.8745E+02	5.0636E+02	4.8781E+02	Not available	Not available	4.8752E+02	4.7639E+02
10	4.5109E+05	7.8558E+05	4.5391E+05	4.5116E+05	4.5115E+05	4.5116E+05	4.3922E+05
11	1.7919E+16	1.5527E+15	1.9593E+16	1.7922E+16	1.7925E+16	1.7916E+16	1.7448E+16

[a] Read as 4.2781×10^1.

Table 7. A comparison of reactor transients with reactivity $\rho = 0.1t - 10^{-13} \int_0^t N(t')\, dt'$ by three different methods.

Time	Δt			Time	Δt		
	0.01	0.001	0.0001		0.01	0.001	0.0001
	(a) 3.647 413E+1	2.570 479E+1	2.482 902E+1		(a) 7.022 039E+8	1.432 669E+10	1.436 654E+10
0.1	(b) 3.647 414E+1	2.570 469E+1	2.482 925E+1	0.45	(b) 7.553 930E+9	1.624 986E+10	1.475 784E+10
	(c) 3.647 414E+1	2.570 469E+1	2.482 925E+1		(c) 7.553 930E+9	1.624 986E+10	1.475 784E+10
	(a) 2.702 590E+4	1.239 887E+4	1.147 786E+4		(a) 1.466 456E+9	9.993 182E+9	9.955 653E+9
0.15	(b) 2.702 593E+4	1.239 866E+4	1.147 635E+4	0.5	(b) 9.736 886E+9	8.128 389E+9	9.678 249E+9
	(c) 2.702 593E+4	1.239 866E+4	1.147 635E+4		(c) 9.736 886E+9	8.128 389E+9	9.678 249E+9
	(a) 2.826 209E+9	8.287 527E+8	7.336 549E+8		(a) 1.837 974E+10	1.145 603E+10	1.146 433E+10
0.2	(b) 2.809 975E+9	8.284 594E+8	7.333 822E+8	0.6	(b) 9.629 178E+9	1.137 569E+10	1.149 131E+10
	(c) 2.809 975E+9	8.284 594E+8	7.333 822E+8		(c) 9.629 178E+9	1.137 569E+10	1.149 132E+10
	(a) 2.524 568E+8	1.097 473E+9	1.164 062E+9		(a) 9.641 320E+9	9.761 114E+9	9.764 145E+9
0.25	(b) 1.052 509E+9	1.490 213E+9	1.203 129E+9	0.7	(b) 1.023 336E+10	1.004 924E+10	9.795 691E+9
	(c) 1.052 509E+9	1.490 213E+9	1.203 129E+9		(c) 1.023 336E+10	1.004 924E+10	9.795 693E+9
	(a) 2.889 617E+8	8.184 253E+8	8.166 009E+8		(a) 9.015 225E+9	1.008 927E+10	1.008 607E+10
0.3	(b) 9.501 868E+8	9.061 560E+8	8.254 459E+8	0.8	(b) 1.014 411E+10	1.004 058E+10	1.007 777E+10
	(c) 9.501 868E+8	9.061 560E+8	8.254 459E+8		(c) 1.014 411E+10	1.004 058E+10	1.007 777E+10
	(a) 3.494 661E+8	1.410 910E+9	1.409 498E+9		(a) 1.045 903E+10	1.015 374E+10	1.015 353E+10
0.35	(b) 4.389 950E+9	1.740 204E+9	1.439 587E+9	0.9	(b) 1.011 697E+10	1.014 071E+10	1.015 229E+10
	(c) 4.389 950E+9	1.740 204E+9	1.439 587E+9		(c) 1.011 697E+10	1.014 071E+10	1.015 229E+10
	(a) 4.598 494E+8	3.744 299E+9	3.750 430E+9		(a) 1.018 628E+10	1.010 474E+10	1.010 441E+10
0.4	(b) 1.799 477E+10	5.685 998E+9	3.912 651E+9	1.0	(b) 1.011 392E+10	1.010 907E+10	1.010 485E+10
	(c) 1.799 477E+10	5.685 998E+9	3.912 651E+9		(c) 1.011 393E+10	1.010 907E+10	1.010 485E+10
					(a) 1.003 130E+10	1.003 068E+10	1.002 987E+10
				5.0	(b) 1.002 926E+10	1.002 975E+10	1.002 976E+10
					(c) 1.002 926E+10	1.002 975E+10	1.002 976E+10

(a) The mean of the summation of the reactor response over the entire interval of integration.
(b) Simpson's rule.
(c) Trapezoidal rule.

represented by a linear expression over the appropriate time interval(s) is clearly valid as long as Δt is kept small. However, as subject to this limitation it is desirable to keep Δt reasonably
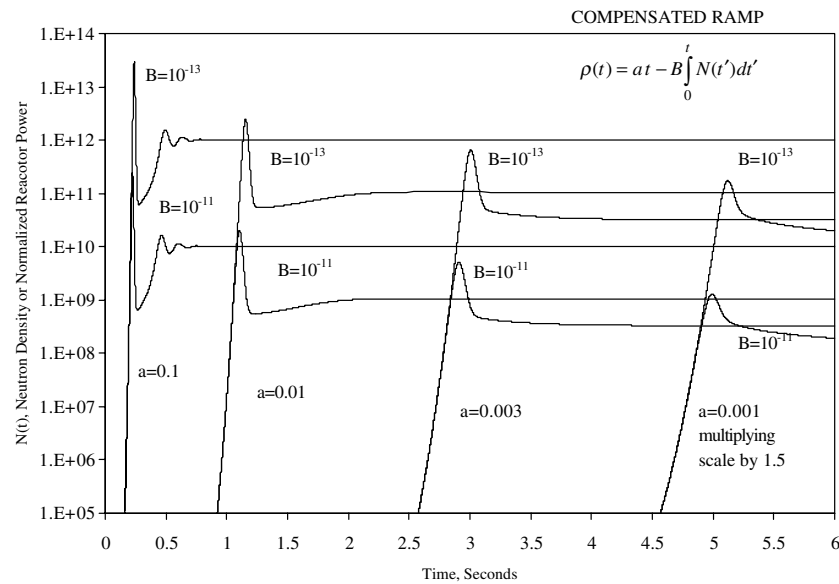
Figure 4. Compensated response to ramp function reactivity changes in U^{235} systems with prompt neutron generation time $= 5 \times 10^{-5}$ s and shutdown coefficients in the range $B = 10^{-11}$ cm^3 s^{-1} to 10^{-13} cm^3 s^{-1}.

Table 8. The CPU time of calculations for the different cases; all the calculations were done under the same conditions.

Functions	CPU (s)	Functions	CPU (s)
$f_{0,1}$	2.41	$f_{2,2}$	5.05
$f_{1,1}$	3.62	$f_{3,2}$	5.65
$f_{2,1}$	4.28	$f_{0,3}$	5.10
$f_{3,1}$	5.05	$f_{1,3}$	5.27
$f_{0,2}$	2.63	$f_{2,3}$	5.93
$f_{1,2}$	4.39	$f_{3,3}$	6.81

large to reduce the number of computed points, minimize possible round-off error, etc. Table 7 compares the results of reactor transients with reactivity feedback by three methods ((a), (b) and (c)) at different transients and times. At a small time step $\Delta t = 0.0001$, typical results for the three cases are reported, while a parallel behaviour of methods (b) and (c) (numerical methods) is obtained at a large time step. The accurate results are achieved by taking the mean of the summation of the reactor response over the entire interval of integration, method (a), table 7. Typical compensated response calculations using the AIM code are illustrated in figure 4. The results in this figure are self-limiting excursions produced by ramp function additions of reactivity in ^{235}U–graphite systems [3, 16] characterized by prompt neutron generation times in the region of 5×10^{-5} s, and B values ranging between 10^{-11} and 10^{-13} cm^3 s^{-1}. The $N(t)$ variations are plotted in figure 4 and exhibit a characteristic damped oscillatory approach to an equilibrium power level at which the rate of reactivity compensation due to (adiabatic) temperature increases to just balance the rate of external reactivity addition.

5. Conclusions

A time-dependent reactivity inserted into a point reactor is coupled multiplicatively with the neutron density to form a set of linear equations with time-dependent coefficients. In the present work we have developed a new AIM (analytical inversion method), applied it to a variety of problems and compared it to a number of other methods. It not only can employ much larger time increment steps due to the stiffness confinement, but also computes rapidly for a given time step due to its completely analytic formulation. The repeated use of the solution in successive time intervals has been shown to save considerable computing time. The approach considered here is based on a combination of numerical analysis tools, including Padé approximations and analytical continuation to the complex plane. Numerical tests show that the technique is both efficient and accurate to several significant figures.

Although the primary application was to the problem of reactor kinetics, the methodology used is more general. The developed method has the ability to reproduce all features of the transients in the solutions. The formalism is applicable equally well to non-linear problems, where the reactivity depends on the neutron density through temperature and thermal hydraulic reactivity feedback.

The computing time (CPU) required for each case has been estimated and is dependent on the number of arithmetic operations. Moreover, this time increases rapidly particularly for the case of varying reactivity when such inversion needs to be done at every time step. Table 8 shows the CPU time of the calculations for different types of Padé rational approximations.

The purification method for the approximate expressions of the exponential function and the explicit treatment of the most dominant roots give a large correction for the Padé approximations. The results for selected times during the transient and for several values of the time step size used in the calculations are shown within the reactivity interval $(-1\$, +1\$)$ for both types of reactors. The RPEs results for both treated and untreated most effective roots, tables 3 and 4, show a large correction effect by automatic inclusion of the roots.

The formalism was applied to the other types of reactivity ramp input and periodical reactivity changes and compared to the results of those obtained using other methods. The AIM is applicable equally well to non-linear problems, where the reactivity depends on the neutron density through temperature reactivity. The best results have been obtained by automatic inclusion of the most effective roots in the basic approximations for these types of reactivity.

It could be concluded that the AIM method for the solution of the point kinetics equations is more elegant, more general and more powerful than the other conventional methods. The applicability of the formalism could be further extended to spacetime kinetics problems.

Appendix

The analytical inversion method is based on an expression for the inverse of $[\mathbf{I} - \varepsilon\mathbf{A}]$, where ε is a scalar. This expression is

$$[\mathbf{I} - \varepsilon\mathbf{A}]^{-1} = \gamma^{-1}\mathbf{a}\mathbf{b}^T + \mathbf{C}$$

where

$$\gamma = \left[1 - \frac{\varepsilon\rho}{\Lambda} + \varepsilon\sum_{i=1}^{G}\frac{\mu_i}{1 + \varepsilon\lambda_i}\right]$$

$$\mathbf{a} = \mathrm{col}\left[1 \quad \frac{\varepsilon\mu_1}{1+\varepsilon\lambda_1} \quad \frac{\varepsilon\mu_2}{1+\varepsilon\lambda_2} \quad \cdots \quad \frac{\varepsilon\mu_G}{1+\varepsilon\lambda_G}\right]$$

$$\mathbf{b} = \mathrm{col}\left[1 \quad \frac{\varepsilon\lambda_1}{1+\varepsilon\lambda_1} \quad \frac{\varepsilon\lambda_2}{1+\varepsilon\lambda_2} \quad \cdots \quad \frac{\varepsilon\lambda_G}{1+\varepsilon\lambda_G}\right]$$

and

$$\mathbf{C} = \mathrm{Diag}\left[0 \quad \frac{1}{1+\varepsilon\lambda_1} \quad \frac{1}{1+\varepsilon\lambda_2} \quad \frac{1}{1+\varepsilon\lambda_3} \quad \cdots \quad \frac{1}{1+\varepsilon\lambda_G}\right].$$

Similarly, we can define $[\mathbf{I} - \bar{\varepsilon}\mathbf{A}]^{-1} = \bar{\gamma}^{(-1)}\overline{\mathbf{a}\mathbf{b}}^T + \overline{\mathbf{C}}$, where $\overline{\gamma}$, $\overline{\mathbf{a}}$, $\overline{\mathbf{b}}$ and $\overline{\mathbf{C}}$ are the complex conjugates of γ, $\mathbf{a}$, $\mathbf{b}$ and $\mathbf{C}$, respectively. For a complex conjugate pair, we consider the pair of factors:

$$[I - \varepsilon A]^{-1}[I - \bar{\varepsilon}A]^{-1} = [I - 2\,\mathrm{Re}(\varepsilon)A + |\varepsilon|^2 A^2]^{-1}$$

which is a real matrix and has a real inverse. This expression can be expressed in the general form as

$$[I - \varepsilon A]^{-1}[I - \bar{\varepsilon}A]^{-1} = (\gamma\overline{\gamma})^{-1}F + Q.$$

For generality, assume that $\varepsilon = \alpha + i\eta$ and $\bar{\varepsilon} = \alpha - i\eta$, where α and η are real constants and $i = \sqrt{-1}$, so that

$$\gamma\bar{\gamma} = 1 - \frac{2\alpha\rho}{\Lambda} + \left(\frac{r\rho}{\Lambda}\right)^2 + \sum_{j=1}^{G} 2\mu_j p_j(\alpha + r^2\lambda_j) - \frac{r^2\rho}{\Lambda}\sum_{j=1}^{G} 2\mu_j p_j(1 + \alpha\lambda_j)$$

$$+ r^2\left(\sum_{j=1}^{G}\mu_j p_j\right)^2 + 2\alpha r^2\left(\sum_{j=1}^{G}\mu_j p_j\right)\left(\sum_{j=1}^{G}\mu_j p_j\lambda_j\right) + r^4\left(\sum_{j=1}^{G}\mu_j p_j\lambda_j\right)^2$$

where $r^2 = \alpha^2 + \eta^2$, $p_j^{-1} = \left(1 + 2\alpha\lambda_j + r^2\lambda_j^2\right)$, $j = 1, \ldots, G$ and $s^2 = \alpha^2 - \eta^2$. The elements of the matrix $F = [f_{kl}]$ can be written as

$$f_{11} = 1 + r^2\sum_{j=1}^{G}\mu_j\lambda_j p_j$$

$$f_{1\,l+1} = \lambda_l p_l\left\{2\alpha + r^2\left(\lambda_l - \frac{\rho}{\Lambda} + \sum_{j=1}^{G}\mu_j p_j\right) + r^2(2\alpha + r^2\lambda_l)\sum_{j=1}^{G}\mu_j\lambda_j p_j\right\}$$

$$f_{k+1\,1} = \mu_k p_k\left\{2\alpha + r^2\left(\lambda_k - \frac{\rho}{\Lambda} + \sum_{j=1}^{G}\mu_j p_j\right) + r^2(2\alpha + r^2\lambda_k)\sum_{j=1}^{G}\mu_j\lambda_j p_j\right\}$$

$$f_{k+1\,l+1} = \mu_k\lambda_l p_k p_l\left\{2s^2 + r^2\left(\begin{array}{c}1 + 2\alpha(\lambda_k + \lambda_l) + r^2\lambda_k\lambda_l - \frac{\rho}{\Lambda}(2\alpha + r^2(\lambda_k + \lambda_l)) \\[4pt] + (2\alpha + r^2(\lambda_k + \lambda_l))\sum\limits_{j=1}^{G}\mu_j p_j + (2s^2 + r^2) \\[4pt] + 2\alpha r^2(\lambda_k + \lambda_l) + r^4\lambda_k\lambda_l)\sum\limits_{j=1}^{G}\mu_j\lambda_j p_j\end{array}\right)\right\}$$

where $k = 1, 2, \ldots, G$ and $l = 1, 2, \ldots, G$ and matrix Q can be written as

$$Q = \mathrm{diag}\,[0 \quad p_1 \quad p_2 \quad \cdots \quad p_G].$$

References

[1] Aboanber A E and Nahla A A 2002 *J. Phys. A: Math. Gen.* **35** 3245–63
[2] Hetrick D L 1971 *Dynamics of Nuclear Reactors* (Chicago, IL: University of Chicago Press)
[3] Keepin G R 1965 *Physics of Nuclear Kinetics* (Reading, MA: Addison-Wesley)
[4] Chao Y A and Attard A 1985 *Nucl. Sci. Eng.* **90** 40
[5] Sanchez J 1989 *Nucl. Sci. Eng.* **103** 94
[6] Frohlich R and Johnson S R 1969 *Nucleonik* **12** 93
[7] Russel V K and Duncan D L 1982 *Trans. Am. Nucl. Soc.* **43** 714
[8] Gupta H B and Trasi M S 1986 *Ann. Nucl. Energy* **13** 203–7
[9] March-Leuba J *et al* 1986 *Nucl. Sci. Eng.* **93** 111–23
[10] Keepin G R and Cox C 1965 *Nucl. Sci. Eng.* **8** 670–90
[11] Clark M and Hansen K F 1964 *Numerical Methods of Reactor Analysis* (New York: Academic)
[12] Plaston A and Rabinowitz P 1978 *First Course in Numerical Analysis* (New York: McGraw-Hill)
[13] Plybon B F 1992 *An Introduction to Applied Numerical Analysis* (Boston, MA: PWS-KENT Publishing Company)
[14] Nishigori T 1991 *Nucl. Sci. Eng.* **108** 347–54
[15] Porsching T A 1966 The numerical solution of the reactor kinetics equations by difference analogs: a comparison of methods *WAPD-TM-564*, US National Bureau of Standards, US Department of Commerce
[16] Yeh Kueng 1978 *Nucl. Sci. Eng.* **66** 235–42